




Syntheses, crystal structures, and luminescent properties of three metal coordination polymers based on adipic acid and 2-(pyridine-3-yl)-(1H)-benzimidazole

Cui-Cui Wang, Jin-Hua Wang, Gui-Mei Tang, Yong-Tao Wang, Yue-Zhi Cui & Seik Weng Ng


To cite this article: Cui-Cui Wang, Jin-Hua Wang, Gui-Mei Tang, Yong-Tao Wang, Yue-Zhi Cui & Seik Weng Ng (2015) Syntheses, crystal structures, and luminescent properties of three metal coordination polymers based on adipic acid and 2-(pyridine-3-yl)-(1H)-benzimidazole, Journal of Coordination Chemistry, 68:21, 3918-3931, DOI: [10.1080/00958972.2015.1084418](https://doi.org/10.1080/00958972.2015.1084418)

To link to this article: <http://dx.doi.org/10.1080/00958972.2015.1084418>

 View supplementary material 

 Accepted author version posted online: 21 Aug 2015.
Published online: 14 Sep 2015.

 Submit your article to this journal 

 Article views: 68

 View related articles 

 View Crossmark data 

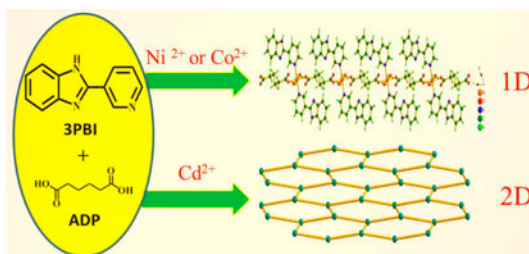
Syntheses, crystal structures, and luminescent properties of three metal coordination polymers based on adipic acid and 2-(pyridine-3-yl)-(1*H*)-benzimidazole

CUI-CUI WANG[†], JIN-HUA WANG[†], GUI-MEI TANG^{*†}, YONG-TAO WANG^{*†}
YUE-ZHI CUI[†] and SEIK WENG NG[‡]

[†]Shandong Provincial Key Laboratory of Fine Chemicals, Department of Chemical Engineering, Qilu University of Technology, Jinan, China

[‡]Department of Chemistry, University of Malaya, Kuala Lumpur, Malaysia

(Received 6 May 2015; accepted 27 July 2015)



Three new metal coordination polymers constructed from adipic acid and 2-(pyridin-3-yl)-(1*H*)-benzimidazole ligands, $[M(\text{ADP})(3\text{PBI})_2(\text{H}_2\text{O})_2] \cdot 2\text{H}_2\text{O}$ ($M = \text{Ni}$ and Co for **1** and **2**, respectively) and $[\text{Cd}(\text{ADP})(3\text{PBI})(\text{H}_2\text{O})]$ (**3**) [ADP = adipic acid dianion; 3PBI = 2-(pyridin-3-yl)-(1*H*)-benzimidazole], have been synthesized by hydrothermal reactions and were characterized by X-ray single-crystal diffraction, elemental analyses, IR, powder X-ray diffraction, and thermogravimetry. Complexes **1** and **2** are isostructural. Both form a 1-D linear chain structure, which is further assembled into a 3-D supramolecular framework by $\pi \cdots \pi$ stacking and hydrogen bonding interactions. Complex **3** possesses a binuclear unit and displays a 2-D layer which is further extended to a 3-D supramolecular architecture via hydrogen bonding and other weak packing interactions. The luminescent properties of **3** were investigated in the solid state at room temperature.

Keywords: Hydrothermal reaction; 2-(Pyridin-3-yl)-(1*H*)-benzimidazole; Adipic anion; Luminescence

1. Introduction

The design and construction of metal coordination polymers (MCPs) have received attention owing to their potential applications as functional materials for gas storage and separation [1–7], drug delivery [8, 9], catalysis [10, 11], nonlinear optics [12], magnetic materials [13, 14], sensing [15, 16], luminescence [17, 18], and ferroelectricity [19, 20]. Metal ions

*Corresponding authors. Email: meiguit@qlu.edu.cn (G.-M. Tang); ceswyt@qlu.edu.cn (Y.-T. Wang)

and the ligands are crucial for the structural architectures and functionalities of MCPs as the structures and properties of these complexes are influenced by the coordination geometries of metal ions, the flexibility, shape, symmetry, and substituent groups of ligands [21]. Auxiliary bis-carboxylate ligands can also influence the structures of MCPs, satisfying charge balance, mediating the coordination geometries of metal centers [22–27], and providing diverse coordination modes [28, 29]. Construction of diverse architectures as potential candidates for functional materials remains a challenge.

Numerous MCPs with aliphatic dicarboxylate ligands and *N*-heteroaromatic ligands have been developed. The flexibility and conformational freedom of aliphatic dicarboxylate ligands gives a variety of interesting structural motifs and $\pi\cdots\pi$ stacking interactions among *N*-heteroaromatic ligands, which play very important roles in the construction of MCPs with interesting supramolecular architectures [30]. Therefore, the synthesis of low dimensional structures through self-assembly is still a challenge [31–34].

Recently, we designed and synthesized a functional ligand **3PBI** (2-(pyridin-3-yl)-(1*H*)-benzimidazole), which is a good choice to construct coordination polymers. **3PBI** is one kind of ligand containing a *N*-heterocyclic group, and possesses the following specific features: (1) It has three *N*-donors which can take part in coordinating with a metal ion, and act as donor and acceptor of hydrogen bonds. (2) There exist three types of aromatic rings, pyridine, phenyl, and imidazole, which can conveniently form $\pi\cdots\pi$ stacking interactions. Additionally, auxiliary bis-carboxylate ligands can provide charge balance and mediate the coordination geometries of metal centers and even can provide versatile coordination modes, which influence the final structures of MCPs. Combining the benefits of bis-carboxylate ligands and rigid ligands, we chose **3PBI** and adipic acid ligands to produce metal–organic architectures with different structural motifs. Herein, we report the synthesis, structures, and luminescence of three new MCPs, $[\mathbf{M}(\mathbf{ADP})(\mathbf{3PBI})_2(\text{H}_2\text{O})_2]\cdot 2\text{H}_2\text{O}$ ($\mathbf{M} = \text{Ni}$ and Co for **1** and **2**, respectively), and $[\text{Cd}(\mathbf{ADP})(\mathbf{3PBI})(\text{H}_2\text{O})]$ (**3**) [\mathbf{ADP} = adipic acid dianion, **3PBI** = 2-(pyridin-3-yl)-(1*H*)-benzimidazole], which have been obtained under hydrothermal conditions. Additionally, their thermogravimetric analyses (TGA) are also discussed.

2. Experimental

2.1. Materials and measurements

Nicotinic acid was purchased from Tian Jin GuangFu Fine Chemical Research Institute. 1, 2-Phenylene diamine and adipic acid were purchased from Sinopharm Chemical Reagent Limited Corporation. Sodium hydroxide was purchased from Tian Jin Guang Cheng Chemical Reagent Limited Corporation. Nickel sulfate, cobalt sulfate, and cadmium sulfate were obtained from Tian Jin Fu Chen Chemical Reagent Factory, Shang Hai Shi Yi Chemical Reagent Limited Corporation, and Shang Hai Chemical Reagent Corporation, respectively. Dimethylformamide (DMF) and polyphosphoric acid (PPA) were purchased from Aladdin Industrial Corporation. 2-(Pyridin-3-yl)-(1*H*)-benzimidazole (**3PBI**) was synthesized according to literature procedures [35]. The reagents and solvents employed were used as received. Elemental analyses were performed on an Elementar vario EL III microanalyser. FT-IR spectra were recorded as KBr pellets from 400 to 4000 cm^{-1} on a Bruker spectrometer. Powder X-ray diffraction (PXRD) was recorded on a Bruker D8 Avance diffractometer at 40 kV, 40 mA with a Cu-target tube and a graphite monochromator; 2θ falls in the range of 5–60°.

The experimental PXRD patterns are in agreement with the corresponding simulated ones except for the relative intensity variation because of the preferred orientations of the crystals. Therefore, the phase purity of the as-synthesized products is substantiated. At room temperature, solid-state fluorescent studies were conducted on a HITACHI F-4600 system. TGA data were collected with a TA SDT Q600 analyzer in N₂ at a heating rate of 10 °C min⁻¹ from 30 to 700 °C.

2.2. Synthesis of **3PBI** (2-(pyridin-3-yl)-(1H)-benzimidazole)

To a mixture of solid nicotinic acid (1.354 g, 0.011 mol) and 1,2-phenylene diamine (1.081 g, 0.010 mol), which was ground and mixed adequately, polyphosphoric acid (10 mL) was added. The reaction mixture was intermittently heated under microwave irradiation. Subsequently, two blocks of ice were added. The reaction mixture was cooled to room temperature and then poured into water (30 mL). The pH of the reaction mixture was adjusted to 7 by adding 10% NaOH solution. The solid formed was collected and crystallized from pure water to give yellow needle-like crystals. Yield (76.7%, 1.496 g). M.p. 263–269 °C. Microanalyses of **3PBI** are in accord with that reported previously [36–38].

2.3. Synthesis of [Ni(ADP)(**3PBI**)₂(H₂O)₂]·2H₂O (**1**)

A reaction mixture of NiSO₄·6H₂O (0.0260 g, 0.1 mmol), **3PBI** (0.0195 g, 0.1 mmol), NaOH (0.0072 g, 0.18 mmol), **ADP** (0.0146 g, 0.1 mmol), and water (6 mL) was added to a 15-mL Teflon reactor and heated under autogenous pressure at 160 °C for 3 days. The reaction mixture was cooled to room temperature at a rate of 5 °C h⁻¹. Green pellet crystals of **1** suitable for X-ray diffraction analysis were obtained (0.032 g, yield: 48.01% based on NiSO₄). Elemental analysis Calcd (%) for C₃₀H₃₄NiN₆O₈ (665.34): C, 54.16; H, 5.15; N, 12.63; found: C, 54.40; H, 5.17; N, 12.57; IR (KBr, cm⁻¹): 3359(w), 3203(w), 2926(w), 2220(br), 1552(s), 1448(m), 1404(s), 1313(s), 1286(m), 1286(m), 1226(m), 1195(m), 1128(m), 1055(w), 1028(w), 1001(w), 962(m), 735(s), 690(m), 432(m), 408(w).

2.4. Synthesis of [Co(ADP)(**3PBI**)₂(H₂O)₂]·2H₂O (**2**)

A reaction mixture of CoSO₄·6H₂O (0.0280 g, 0.1 mmol), **3PBI** (0.0195 g, 0.1 mmol), NaOH (0.0072 g, 0.18 mmol), **ADP** (0.0146 g, 0.1 mmol), water (6 mL), and DMF (3 mL) was added to a 15-mL Teflon reactor and heated under autogenous pressure at 160 °C for 3 days. The reaction mixture was cooled to room temperature at a rate of 5 °C h⁻¹. Red pellet crystals of **2** suitable for single X-ray diffraction analysis were obtained (0.008 g, yield: 12.02% based on CoSO₄). Elemental analysis Calcd (%) for C₃₀H₃₄CoN₆O₈ (665.56): C, 54.14; H, 5.15; N, 12.63; found: C, 55.54; H, 5.10; N, 12.68; IR (KBr, cm⁻¹): 3020(w), 2862(w), 2790(w), 2502(w), 1593(s), 1460(w), 1439(w), 1344(m), 1028(m), 892(w), 802(s), 739(w), 407(w).

2.5. Synthesis of [Cd(ADP)(**3PBI**)(H₂O)] (**3**)

CdSO₄·3/8 H₂O (0.026 g, 0.1 mmol), **3PBI** (0.0195 g, 0.1 mmol), NaOH (0.0072 g, 0.18 mmol), adipic acid (0.0146 g, 0.1 mmol), and water (6 mL) were added to a 15-mL Teflon reactor and heated under autogenous pressure at 160 °C for 3 days. The reaction

mixture was cooled to room temperature at a rate of 5 °C h⁻¹. Yellow pellet crystals of **3** suitable for X-ray diffraction analysis were obtained (0.0123 g, yield: 27% based on CdSO₄). Elemental analysis Calcd (%) for C₁₈H₁₅Cd N₃O₅ (465.73): C, 46.38; H, 3.22; N, 9.02; found: C, 46.19; H, 3.24; N, 9.05. IR (KBr, cm⁻¹): 2943(w), 1557(s), 1419(s), 1329(m), 1278(m), 1197(m), 1130(w), 1049(m), 962(m), 930(m), 816(m), 740(s), 700(m), 637(m), 519(w), 428(m).

2.6. Single-crystal structure determination

Single-crystal structure determinations of **3PBI** and three complexes were measured by an Agilent Technologies SuperNova Dual diffractometer equipped with a graphite monochromator and Mo K α radiation ($\lambda = 0.71073$ Å). The lattice parameters were obtained by least-squares refinement of the diffraction data. All the measured independent reflections were used in the structural analysis, and semi-empirical absorption corrections were applied using the CrysAlis PRO program [39]. SAINT was used for integration of the diffraction profiles [40]. The structure was solved by direct methods using the SHELXS program of the SHELXTL package and refined with SHELXL [41, 42]. All non-hydrogen atoms were located in successive difference Fourier syntheses. The final refinement was performed by full-matrix least-squares methods with anisotropic thermal parameters for all the non-hydrogen atoms based on F^2 . Except for hydrogen bonded to oxygen, hydrogens were first found in difference electron density maps, and then placed in calculated sites and included in the final refinement in the riding model approximation with displacement parameters derived from the parent atoms to which they were bonded. Special computations for the crystal

Table 1. Crystal data and structure refinement parameters for **3PBI** and **1–3**.

Compound reference	3PBI	1	2	3
Chemical formula	C ₁₂ H ₉ N ₃	C ₃₀ H ₃₄ N ₆ NiO ₈	C ₃₀ H ₃₄ CoN ₆ O ₈	C ₁₈ H ₁₅ CdN ₃ O ₅
Formula mass	195.22	665.34	665.56	465.73
Crystal system	Monoclinic	Triclinic	Triclinic	Monoclinic
<i>a</i> (Å)	10.1952(6)	8.8181(4)	8.8520(4)	10.3656(6)
<i>b</i> (Å)	11.4311(6)	9.7023(8)	9.7334(6)	22.8865(19)
<i>c</i> (Å)	17.2491(9)	9.7404(9)	9.7482(5)	7.7754(4)
α (°)	90.00	61.154(9)	61.221(6)	90.00
β (°)	103.490(6)	86.030(5)	87.843(4)	94.931(5)
γ (°)	90.00	88.029(5)	85.846(4)	90.00
Unit cell volume (Å ³)	1954.79(18)	728.19(10)	734.23(7)	1837.7(2)
Temperature (K)	100(2)	100(2)	100(2)	100(2)
Space group	<i>P</i> 2 ₁ / <i>n</i>	<i>P</i> -1	<i>P</i> -1	<i>P</i> 2 ₁ / <i>c</i>
No. of formula units per unit cell, <i>Z</i>	8	1	1	4
Radiation type	MoK α	MoK α	MoK α	MoK α
Absorption coefficient μ (mm ⁻¹)	0.083	0.730	0.647	1.223
No. of reflections measured	9908	6219	13,347	8973
No. of independent reflections	4508	3358	3395	4222
<i>R</i> _{int}	0.0275	0.0312	0.0359	0.0512
Final <i>R</i> ₁ values [<i>I</i> > 2 σ (<i>I</i>)] ^a	0.0565	0.0485	0.0304	0.0538
Final <i>wR</i> (<i>F</i> ²) values [<i>I</i> > 2 σ (<i>I</i>)]	0.1383	0.1096	0.0687	0.1150
Final <i>R</i> ₁ values (all data)	0.0706	0.0540	0.0363	0.0849
Final <i>wR</i> (<i>F</i> ²) values (all data) ^b	0.1495	0.1131	0.0738	0.1349
Goodness of fit on <i>F</i> ²	1.026	1.178	1.027	1.052
CCDC number	1,061,857	994,668	994,669	994,670

$$^a R_1 = \frac{\sum ||F_o| - |F_c||}{\sum |F_o|}$$

$$^b wR_2 = \frac{[\sum [w(F_o^2 - F_c^2)^2]]}{\sum [w(F_o^2)^2]}^{1/2}$$

structure discussions were carried out with PLATON for Windows [43]. A summary of the crystallographic data and structure refinements is listed in table 1. Selected bond lengths and angles are given in table 2. Corresponding hydrogen bonding data for **3PBI** and **1–3** are listed in table 3.

3. Results and discussion

3.1. Description of the crystal structure

3.1.1. Structure description of ligand 3PBI. Single-crystal X-ray analysis for **3PBI** reveals that it has a mononuclear structure which crystallizes in the form of space group $P2_1/n$. There are two **3PBI** molecules in the asymmetric unit [figure 1(a)]. As shown in figure 1(b), a pair of **3PBI** molecules, each using the carbons from pyridine groups and nitrogens from benzimidazole, forms hydrogen bonds ($C(5)-H(5)\cdots N(5)$, 3.456(2) Å (table 3) in the head–tail pattern [44], through which a dimer structure is generated. Consequently, 1-D hydrogen-bonded chains can be observed along the b axis via another weak hydrogen bond ($C(20)-H(20)\cdots N(3)^c$, 3.468(2) Å, $^c x, -1 + y, z$) [figure 1(b) and table 3].

Table 2. Selected bond lengths (Å) and angles (°) for **1–3**.

1			
Ni(1)–O(1)	2.0614(18)	Ni(1)–O(1W)	2.088(2)
Ni(1)–N(1)	2.100(3)		
O(1)–Ni(1)–O(1W)	87.83(9)	O(1)–Ni(1)–N(1)	90.21(9)
O(1)–Ni(1)–O(1) ^a	180.00	O(1)–Ni(1)–O(1W) ^a	92.17(9)
O(1)–Ni(1)–N(1) ^a	89.79(9)	O(1W)–Ni(1)–N(1)	93.76(11)
O(1W)–Ni(1)–N(1) ^a	86.24(11)	O(1W)–Ni(1)–O(1W) ^a	180.00
N(1)–Ni(1)–N(1) ^a	180.00	O(1) ^a –Ni(1)–N(1) ^a	90.22(9)
2			
Co(1)–O(1)	2.0787(13)	Co(1)–O(1W)	2.1094(11)
Co(1)–N(1)	2.1491(13)		
O(1)–Co(1)–O(1W)	91.46(5)	O(1)–Co(1)–O(1) ^b	180.00
O(1W)–Co(1)–N(1)	93.80(5)	O(1W)–Co(1)–N(1) ^b	86.20(5)
O(1W)–Co(1)–O(1) ^b	88.54(5)	O(1)–Co(1)–N(1)	90.37(5)
N(1)–Co(1)–O(1) ^b	89.63(5)	N(1)–Co(1)–N(1) ^b	180.00
3			
Cd(1)–O(1)	2.377(4)	Cd(1)–O(1W)	2.270(4)
Cd(1)–O(2)	2.355(4)	Cd(1)–N(1)	2.350(4)
Cd(1)–O(3) ^c	2.339(4)	Cd(1)–O(4) ^c	2.465(4)
O(1)–Cd(1)–O(1W)	95.04(14)	O(1)–Cd(1)–O(2)	55.93(14)
O(1)–Cd(1)–N(1)	88.13(15)	O(1)–Cd(1)–O(4) ^d	90.71(13)
O(1)–Cd(1)–O(3) ^c	135.12(13)	O(1)–Cd(1)–O(4) ^c	167.76(12)
O(1W)–Cd(1)–O(2)	106.16(14)	O(1W)–Cd(1)–N(1)	85.44(14)
O(1W)–Cd(1)–O(3) ^c	81.10(14)	O(2)–Cd(1)–N(1)	142.50(15)
O(1W)–Cd(1)–O(4) ^c	94.11(13)	O(1W)–Cd(1)–O(4) ^d	170.83(13)
O(2)–Cd(1)–O(3) ^c	82.05(14)	O(2)–Cd(1)–O(4) ^c	128.57(12)
O(2)–Cd(1)–O(4) ^d	82.97(13)	N(1)–Cd(1)–O(4) ^d	87.62(12)
N(1)–Cd(1)–O(3) ^c	135.41(15)	N(1)–Cd(1)–O(4) ^c	84.51(13)
O(3) ^c –Cd(1)–O(4) ^c	54.62(11)	O(3) ^c –Cd(1)–O(4) ^d	99.81(12)

Symmetry codes:

^a1 – x , 1 – y , 1 – z .

^b1 – x , 1 – y , 1 – z .

^c1 – x , 1/2 + y , 1/2 – z .

^d x , 1/2 – y , –1/2 + z .

Table 3. Hydrogen bond geometries in the crystal structure of **3PBI** and **1–3**, respectively.

Compound	D–H \cdots A ^a	H \cdots A (Å)	D \cdots A (Å)	D–H \cdots A (°)
3PBI	N(2)–H(2) \cdots N(5)	1.993(12)	2.873(2)	176(2)
	C(1)–H(1) \cdots N(4) ^a		3.478(3)	
	N(6)–H(6) \cdots N(1) ^b	2.01(2)	2.836(2)	154(2)
	C(5)–H(5) \cdots N(5)		3.456(2)	
	C(20)–H(20) \cdots N(3) ^c		3.468(2)	
1	N(2)–H(2) \cdots O(2) ^d	2.01(2)	2.847(4)	160(3)
	O(1W)–H(11) \cdots O(2W)	1.89(5)	2.726(4)	173(5)
	O(1W)–H(12) \cdots O(2) ^e	1.90(4)	2.682(4)	155(3)
	O(2W)–H(21) \cdots O(2) ^f	1.97(2)	2.801(3)	177(5)
	O(2W)–H(22) \cdots N(3)	2.01(4)	2.853(5)	174(2)
	C(8)–H(8) \cdots O(2W)		3.392(4)	
	C(14)–H(14) \cdots O(2W) ^g		3.496(5)	
2	N(2)–H(2) \cdots O(2) ^h	2.010(12)	2.8549(17)	161.4(16)
	O(1W)–H(11) \cdots O(2)	1.89(2)	2.6964(19)	158.8(18)
	O(1W)–H(12) \cdots O(2W)	1.88(2)	2.7222(19)	178(3)
	O(2W)–H(21) \cdots N(3)	2.024(16)	2.8605(18)	173(3)
	O(2W)–H(22) \cdots O(2) ⁱ	1.959(13)	2.7976(16)	175.8(16)
	C(8)–H(8) \cdots O(2W)		3.402(2)	
3	N(2)–H(2) \cdots O(2) ^j	1.97(2)	2.820(6)	162(5)
	O(1W)–H(11) \cdots O(3) ^k	1.92(4)	2.707(5)	157(6)
	O(1W)–H(12) \cdots N(3) ^l	1.96(4)	2.793(6)	171(6)
	C(7)–H(7) \cdots O(1)		3.206(7)	
	C(11)–H(11A) \cdots O(4) ^m		3.107(6)	

Symmetry codes:

^a1 + *x*, *y*, *z*.^b1 – *x*, 1 – *y*, 1 – *z*.^c*x*, –1 + *y*, *z*.^d1 – *x*, –*y*, 1 – *z*.^e1 – *x*, 1 – *y*, 1 – *z*.^f1 + *x*, *y*, *z*.^g2 – *x*, 1 – *y*, –*z*.^h*x*, *y*, –1 + *z*.ⁱ2 – *x*, 1 – *y*, 1 – *z*.^j1 – *x*, 1 – *y*, 1 – *z*.^k*x*, 1/2 – *y*, –1/2 + *z*.^l2 – *x*, 1 – *y*, 1 – *z*.^m1 – *x*, 1/2 + *y*, 1/2 – *z*.

Additionally, each **3PBI** using a carbon and the nitrogen from pyridine forms another kind of hydrogen bond (C(1)–H(1) \cdots N(4)^a, 3.478(3) Å, ^a1 + *x*, *y*, *z*). A series of chains along the *b* axis lie parallel to each other and are connected by this kind of hydrogen bond, resulting in a wave-like 2-D hydrogen-bonded network along the crystallographic *ab* plane [figure 1(c) and table 3]. Notably, there exist three weak $\pi\cdots\pi$ (Cg(1) \cdots Cg(2)^a, 3.505(1) Å, ^a1 – *x*, 2 – *y*, 1 – *z*; Cg(5) \cdots Cg(5)^b, 3.6962(11) Å, ^b1 – *x*, 1 – *y*, 1 – *z*) packing interactions between two different benzimidazole groups (Cg(1), Cg(2)) and two identical pyridine groups (Cg(5)). In addition, there exist two other types of hydrogen bonds (N(2)–H(2) \cdots N(5) and N(6)–H(6) \cdots N(1)^b distances of 2.873(2) and 2.836(2) Å, respectively, ^b1 – *x*, 1 – *y*, 1 – *z*) (table 3). The former is constructed through N(2) and N(5) from two different benzimidazole groups; the latter is found through N(6) and N(1) from benzimidazole and pyridine groups, respectively. These supramolecular interactions extend the 2-D layers to a 3-D supramolecule [figure 1(d)].

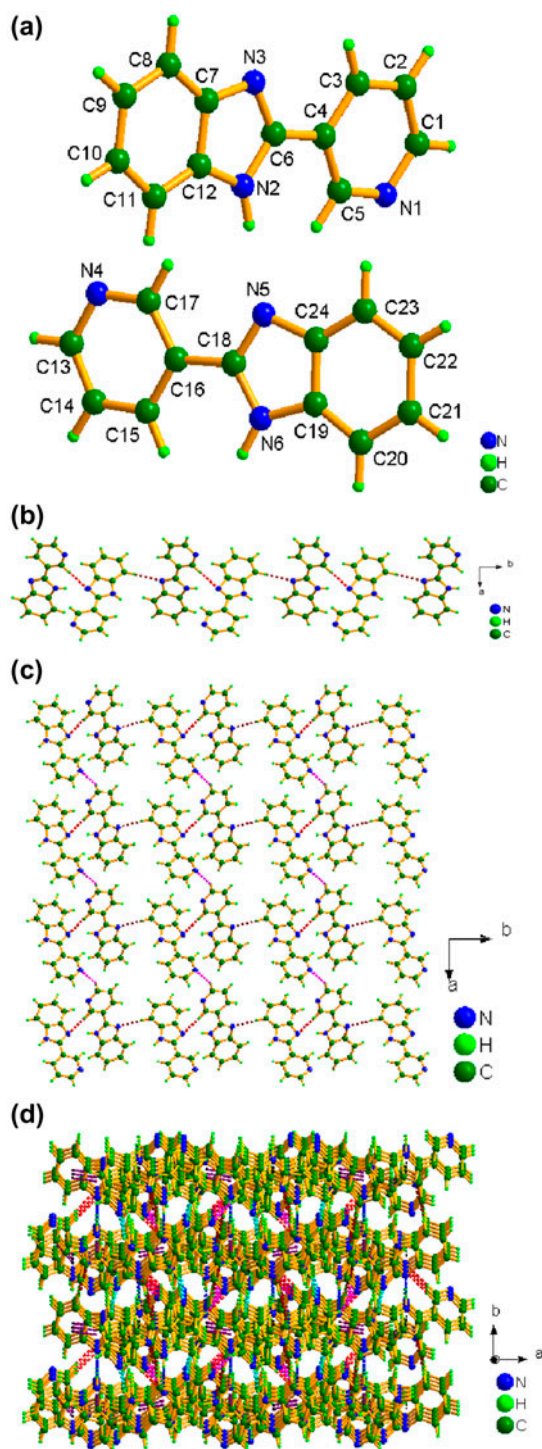


Figure 1. (a) A perspective view of 3PBI. (b) A 1-D chain through hydrogen bonds along the *b* axis. (c) A 2-D supramolecular network formed by hydrogen bonding interactions in 3PBI. (d) The packing diagram of 3PBI.

3.1.2. Structure description of 1 and 2. Single-crystal X-ray analysis reveals that **1** and **2** are isostructural. They are both 1-D polymers and crystallize in the triclinic space group *P*-1. For convenience, the structure of **1** is discussed herein. As shown in figure 2(a), the asymmetric unit is composed of half of a Ni(II) ion, one **3PBI**, half of an **ADP** ligand, one coordinated water, and one free water. The central Ni ion is six-coordinate to two nitrogens from two **3PBI** ligands, two oxygens from two **ADP** ligands, and two water molecules. The coordination geometry can be described in terms of a slightly distorted octahedral configuration. The Ni–O bond distances in **1** range from 2.061(2) to 2.088(2) Å and the Ni–N bond length is 2.100(3) Å (table 2), which is in agreement with those published previously [45]. The bond lengths of Co–O in **2** are 2.0787(13)–2.1094(11) Å, in accord with those published previously [45]. Interestingly, the average bond length of Co–O is 2.086 Å and the bond length of Co–N is 2.1491(13) Å, which are slightly longer than the common Co–O and Co–N distances of 1.94 and 1.96 Å, respectively [45]. The bond angles around the Co are 80.00(11)–180.00°. Thus, each **ADP** is a linear connector, which links two adjacent metal ions. As a result, a 1-D chain is observed [figure 2(b)].

Supramolecular structures mainly depend on three kinds of interactions, coordination bonds, strong hydrogen bonds, and packing interactions. Intermolecular hydrogen bonds are formed between **3PBI** and **ADP** ligands. These bond lengths and angles (N–H···O) are 2.847(4) Å and 160(3)° for **1**, and 2.855(2) Å and 161.4(16)° for **2**, through which 1-D polymeric chains are extended to a 2-D supramolecular layer [figure 2(c)]. We also found three kinds of O–H···O hydrogen bonds and two kinds of C–H···O interactions in **1** and **2** [figure 2(d) and table 3]: (a) There exist O–H···O intermolecular hydrogen bonds between coordinated water and free water. These bond lengths and angles are 2.726(4) Å and 173(5)° for **1**, and 2.722(19) Å and 178(3)° for **2**. (b) O–H···O intermolecular hydrogen bonds form between oxygens from the coordinated water and oxygens from **ADP**. These bond lengths and angles are 2.682(4) Å and 155(3)° for **1**, and 2.696(2) Å and 158.8(18)° for **2**. (c) O–H···O intermolecular hydrogen bonding occurs between free water molecules and **ADP** ligands. These bond lengths and angles are 2.801(3) Å and 177(5)° for **1**, and 2.7976(16) Å and 175.8(16)° for **2**. (d) Another type of hydrogen bond occurs between free waters and **3PBI** ligands (O(2W)–H(22)···N(3), 2.853(5) Å; C(8)–H(8)···O(2W), 3.392(4) Å; C(14)–H(14)···O(2W)^g, 3.496(5) Å, ^g $x, 1/2 - y, -1/2 + z$) for **1** and (O(2W)–H(21)···N(3), 2.8605(18) Å; C(8)–H(8)···O(2W), 3.402(2) Å for **2**) (table 3).

Apart from these hydrogen bonding interactions, there exist two kinds of weak π ··· π stacking interactions between aromatic rings. One occurs between the imidazole groups and phenyl rings (3.5775 and 3.6560 Å for **1** and **2**, respectively) and another between two phenyl groups (3.6515 and 3.5822 Å for **1** and **2**, respectively). These supramolecular interactions extend the 2-D layers to a 3-D supramolecular architecture, which can support the stability of the stacked arrangement [figure 2(d)].

3.1.3. Structure description of 3. The results of the X-ray crystallographic analysis reveal that **3** is a binuclear structure, and crystallizes in the space group *P*2₁/*c* and displays a 2-D structure of the binuclear units. As shown in figure 3(a), the asymmetric unit contains one cadmium ion, one **3PBI**, one **ADP**, and one coordinated water. Cd1 is seven-coordinate in a slightly distorted pentagonal pyramidal geometry. The basal plane consists of one nitrogen from **3PBI** and four oxygens from three different **ADP** ligands. The axial positions are occupied by water and the carboxylate from one **ADP**. The Cd–O bond distances are 2.270(4)–2.465 Å and the bond length of Cd–N is 2.350(4) Å (table 2), normal values [45]. The

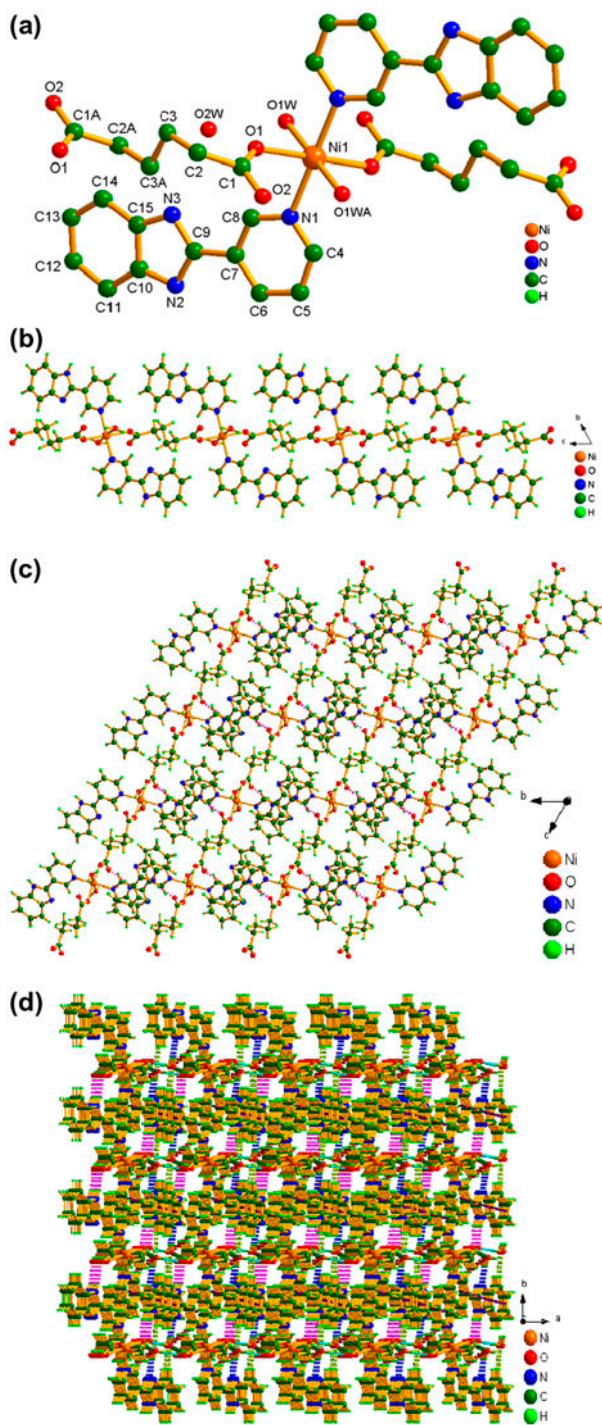


Figure 2. (a) A perspective view of the coordination geometry of Ni(II) in **1** (Co(II) center in **2**). (b) A 1-D chain along the *c* axis in **1**. (c) A 2-D supramolecular network formed by hydrogen bond interactions in **1**. (d) The packing diagram of **1**.

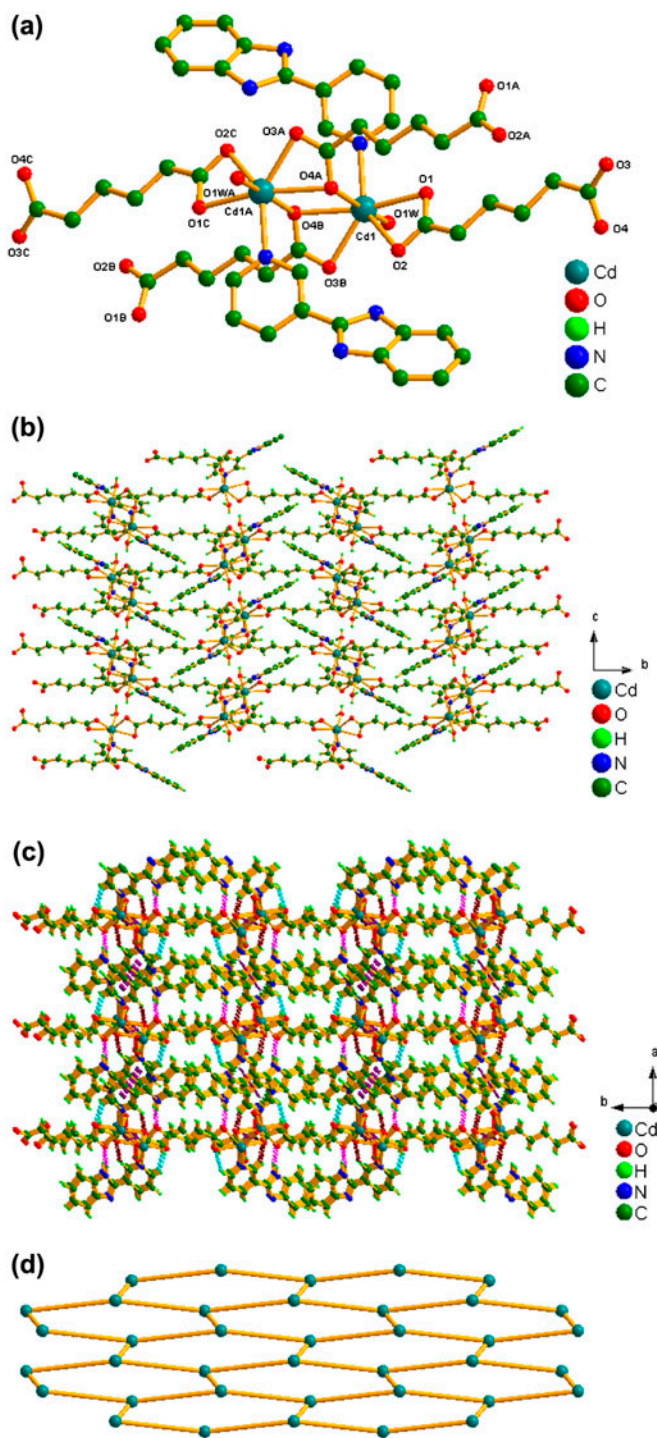


Figure 3. (a) A perspective view of the coordination geometry of the Cd center in **3** and the binuclear structure in **3**. (b) A 2-D layer along the crystallographic *bc* plane. (c) The packing diagram of **3**. (d) The topology structure of **3**.

bond angles of O–Cd–O vary from $54.6(1)^\circ$ to $170.8(1)^\circ$ and the bond angles of O–Cd–N are $84.5(1)$ – $142.5(2)^\circ$. Interestingly, there are two kinds of adipic acid dianion ligands, one is bidentate and the other monodentate. As a result, a binuclear Cd structure is formed [figure 3(a)]. These binuclear units are further extended to a 2-D layer through ADP ligands [figure 3(b)].

The 3-D supramolecular structures mainly originate from hydrogen bonding and packing interactions. Four kinds of hydrogen bonds are observed [figure 3(c) and table 3]: (a) An intermolecular hydrogen bond O–H \cdots O (O(1W)–H(11) \cdots O(3)^h 2.707(5) Å, ^h x , $1/2 - y$, $-1/2 + z$) (table 3) forms between coordinated water and carboxylate of ADP. (b) The intermolecular hydrogen bond N–H \cdots O (N(2)–H(2) \cdots O(2)^g 2.820(6) Å, ^g $1 - x$, $1 - y$, $1 - z$) is generated through nitrogen of 3PBI and oxygen of ADP. (c) Hydrogen bonds of O–H \cdots N (O(1W)–H(12) \cdots N(3)^l 2.793(6) Å, ^l $2 - x$, $1 - y$, $1 - z$) occur between coordinated water and nitrogen of 3PBI. (d) Two intermolecular C–H \cdots O hydrogen bonds are generated between carboxylate groups (C(7)–H(7) \cdots O(1), 3.206(7) Å; C(11)–H(11A) \cdots O(4)^m 3.107(6) Å, ^m $1 - x$, $1/2 + y$, $1/2 - z$).

In addition to these hydrogen bonds, there exist weak $\pi\cdots\pi$ stacking interactions between imidazole rings (3.789(3) Å). Consequently, a 3-D supramolecular architecture is constructed via these hydrogen bonds and weak $\pi\cdots\pi$ packing interactions along the *c* axis [figure 3(c)].

To investigate the topological structure of **3**, Cd(II) ions can be regarded as three connecting nodes, whereas ADP ligands are linear linkers bridging two adjacent Cd(II) ions. Thus, the whole network is simplified to the (6,3) topological structure, as found in some 2-D MCPs [figure 3(d)] [46–48]. The present topological network is a non-uniform topological structure, different from those documented in the literature [49, 50].

3.2. Luminescent properties

Benzimidazole and d^{10} MCPs are known to show good luminescent properties and **3** is composed of benzimidazole groups and cadmium ions, which may display interesting luminescent properties. Hence, the fluorescence emission spectra of **3** were investigated at room

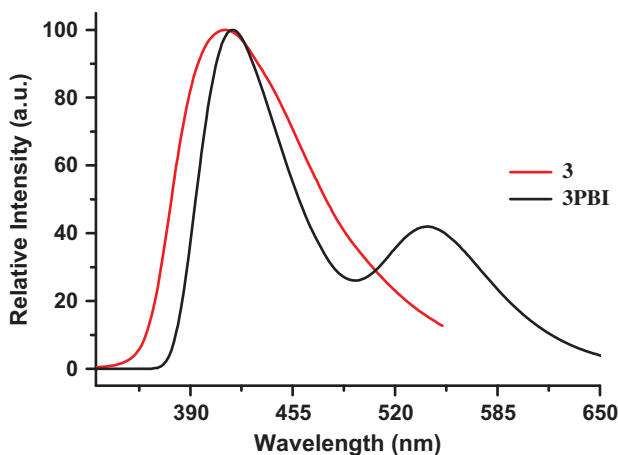


Figure 4. Fluorescent emission spectra of 3PBI and **3** in the solid state at room temperature.

temperature [51, 52]. As shown in figure 4, **3** displays an emission band at 413 nm with excitation at 283 nm. To compare the nature of the emission bands for **3**, we investigated the luminescence properties of free **3PBI** in the solid state at room temperature; two maxima of emission peaks are located at 417 and 541 nm ($\lambda_{\text{ex}} = 283$ nm), respectively. In comparison with **3PBI**, the maximum for **3** is slightly blue-shifted about 5 nm and may be assigned to intraligand $\pi \cdots \pi$ transition [53]. Compared with the organic ligands, the increase in **3** could be a consequence of coordination of the organic ligand to the metal center, which improves the rigidity of the organic ligands, thereby decreasing the loss of energy through a radiationless pathway [54]. These observations suggest that **3** can serve as a candidate for luminescent materials.

3.3. PXRD patterns and TGA

In order to confirm the pure phase of these complexes, their PXRD spectra were examined. As illustrated in figures S1–S3, the peak positions of the simulated and experimental PXRD patterns are in accord with each other. The present results show that products are in a pure phase [55].

To examine the thermal stabilities of **1–3**, TGA were carried out [56]. The experiments were performed on samples consisting of single crystals of **1–3** under a N_2 atmosphere with a heating rate of $10 \text{ }^\circ\text{C min}^{-1}$ (figures 5, S4 and S5). The TGA curve for **1** is similar to that for **2**. The TGA curves show that the first weight loss occurs from 88 to 145 $^\circ\text{C}$ (obsd 11.0%, Calcd 8.1%) for **1** and 86–143 $^\circ\text{C}$ (obsd 10.0%, Calcd 8.1%) for **2**, which corresponds to loss of the free and coordination water. The results indicate that there exist strong hydrogen bonds among the water molecules. The framework collapses from 273 to 694 $^\circ\text{C}$ (obsd 68.0%, Calcd 79.4%) for **1** and 214–693 $^\circ\text{C}$ (obsd 68.0%, Calcd 78.9%) for **2**, showing the departure of organic ligands. The remaining weight is attributed to the final product Ni_2O_3 (obsd 21.0%, Calcd 12.5%) for **1** and Co_2O_3 (obsd 22.0%, Calcd 13.0%) for **2**. The TGA curve of **3** reveals that first weight loss of the coordination water molecules is observed from 121 to 154 $^\circ\text{C}$ (obsd 3.4%, Calcd 3.8%). The second weight loss occurs from 226 to 694 $^\circ\text{C}$ (obsd 77.6%, Calcd 69.2%), showing the departure of organic ligands. The final residual can be assigned to the formation of CdO (obsd 19.0%, Calcd 27.0%) for **3**.

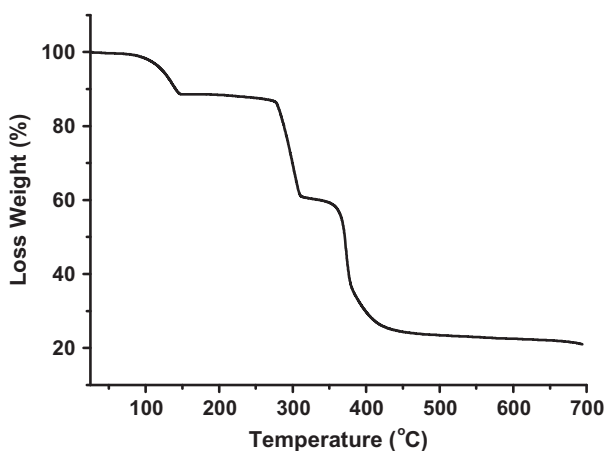


Figure 5. TGA curve of **1**.

4. Conclusion

We obtained three MCPs with different dimensionalities, constructed from transition metal salts with **3PBI** and adipic acid dianion under hydrothermal conditions. There exist a variety of hydrogen bonding and $\pi\cdots\pi$ stacking interactions, through which 3-D supramolecular architectures are constructed. The present work shows that the metal centers and the coordination modes of the bridging ligand play key roles in the final structures. The present results confirm the significant potential of constructing low dimensional structures based on bis-carboxylate and *N*-heterocyclic ligands, providing examples of syntheses of MCPs. Design and development of MCPs based on other bis-carboxylate ligands and *N*-heterocyclic ones are underway at our laboratory.

Acknowledgment

Prof. Yue-Zhi Cui gratefully thanks the National Natural Science Foundation of China [No. 21276149].

Disclosure statement

No potential conflict of interest was reported by the authors.

Funding

This work was financially supported by the Project of Shandong Province Higher Educational Science and Technology Program [grant number J09LB03]; Shandong Distinguished Middle-aged Young Scientist Encouragement and Reward Foundation [grant number BS2011CL034]; and Program for Scientific Research Innovation Team in Colleges and Universities of Shandong Province.

Supplemental data

Supplemental data for this article can be accessed <http://dx.doi.org/10.1080/00958972.2015.1084418>.

References

- [1] S.J. Alesaadi, F. Sabzi. *Int. J. Hydrogen Energy*, **40**, 1651 (2015).
- [2] L.J. Murray, M. Dincă, J.R. Long. *Chem. Soc. Rev.*, **38**, 1294 (2009).
- [3] P. Sarawade, H. Tan, V. Polshettiwar. *ACS Sustainable Chem. Eng.*, **1**, 66 (2013).
- [4] P.Q. Liao, D.D. Zhou, A.X. Zhu, L. Jiang, R.B. Lin, J.P. Zhang, X.M. Chen. *J. Am. Chem. Soc.*, **134**, 17380 (2012).
- [5] H.H. Wu, Q.H. Gong, D.H. Olson, J. Li. *Chem. Rev.*, **112**, 836 (2012).
- [6] J.R. Li, J. Sculley, H.C. Zhou. *Chem. Rev.*, **112**, 869 (2012).
- [7] Z.J. Zhang, Z.Z. Yao, S.C. Xiang, B.L. Chen. *Energy Environ. Sci.*, **7**, 2868 (2014).
- [8] P. Horcajada, R. Gref, T. Baati, P.K. Allan, G. Maurin, P. Couvreur, G. Férey, R.E. Morris, C. Serre. *Chem. Rev.*, **112**, 1232 (2012).
- [9] K. Matsuyama, N. Hayashi, M. Yokomizo, T. Kato, K. Ohara, T. Okuyama. *J. Mater. Chem. B*, **2**, 7551 (2014).
- [10] D.B. Dang, P.Y. Wu, C. He, Z. Xie, C.Y. Duan. *J. Am. Chem. Soc.*, **132**, 14321 (2010).

- [11] J.W. Liu, L.F. Chen, H. Cui, J.Y. Zhang, L. Zhang, C.Y. Su. *Chem. Soc. Rev.*, **43**, 6011 (2014).
- [12] Y.T. Wang, G.M. Tang, W.Z. Wan, Y. Wu, T.C. Tian, J.H. Wang, C. He, X.F. Long, J.J. Wang, S.W. Ng. *CrystEngComm*, **14**, 3802 (2012).
- [13] E. Coronado, G. Minguez Espallargas. *Chem. Soc. Rev.*, **42**, 1525 (2013).
- [14] G.W. Xu, Z.L. Wang, G.X. Wen, S.S. Guo, D.S. Li, J. Zhang. *Inorg. Chem. Commun.*, **55**, 17 (2015).
- [15] L.E. Kreno, K. Leong, O.K. Farha, M. Allendorf, R.P. Van Duyne, J.T. Hupp. *Chem. Rev.*, **112**, 1105 (2012).
- [16] B. Liu. *J. Mater. Chem.*, **22**, 10094 (2012).
- [17] J. Heine, K. Muller Buschbaum. *Chem. Soc. Rev.*, **42**, 9232 (2013).
- [18] M.D. Allendorf, C.A. Bauer, R.K. Bhakta, R.J. Houk. *Chem. Soc. Rev.*, **38**, 1330 (2009).
- [19] C.M. Liu, R.G. Xiong, D.Q. Zhang, D.B. Zhu. *J. Am. Chem. Soc.*, **132**, 4044 (2010).
- [20] T. Hang, W. Zhang, H.Y. Ye, R.G. Xiong. *Chem. Soc. Rev.*, **40**, 3577 (2011).
- [21] Y.G. Ran, J.X. Xie, Y.J. Mu, L.F. Zhang, B. Han. *Inorg. Chim. Acta*, **425**, 17 (2015).
- [22] L. Cheng, W.X. Zhang, B.H. Ye, J.B. Lin, X.M. Chen. *Inorg. Chem.*, **46**, 1135 (2007).
- [23] S.N. Wang, Y.F. Bai, Y.Z. Li, Y. Pan, M. Scheer, X.Z. You. *CrystEngComm*, **9**, 1084 (2007).
- [24] Z.-W. Wang, M. Yu, T. Li, X.-R. Meng. *J. Coord. Chem.*, **66**, 4163 (2013).
- [25] H.L. Wen, W. Wen, D.D. Li, C.B. Liu, M. He. *J. Coord. Chem.*, **66**, 2623 (2013).
- [26] H.P. Xiao, S. Aghabeygi, S.S. Wang, H.-Y. Wu, C.E. Tong, W.B. Zhang, A. Morsali. *J. Coord. Chem.*, **66**, 1821 (2013).
- [27] X. Lu, J. Ye, L. Zhao, Y. Lin, G. Ning. *J. Coord. Chem.*, **67**, 1133 (2014).
- [28] S.Q. Zang, Y. Su, Y.Z. Li, Z.P. Ni, H.Z. Zhu, Q.J. Meng. *Inorg. Chem.*, **45**, 3855 (2006).
- [29] Y. Su, S.Q. Zang, Y.Z. Li, H.Z. Zhu, Q.J. Meng. *Cryst. Growth Des.*, **7**, 1277 (2007).
- [30] E.B. Ying, Y.Q. Zheng, H.J. Zhang. *J. Mol. Struct.*, **693**, 73 (2004).
- [31] J.H. Wang, G.M. Tang, Y.T. Wang, T.X. Qin, S.W. Ng. *CrystEngComm*, **16**, 2660 (2014).
- [32] Y.T. Wang, G.M. Tang, Y.C. Zhang, W.Z. Wan, J.C. Yu, T.D. Li, Y.Z. Cui. *J. Coord. Chem.*, **63**, 1504 (2010).
- [33] Y.T. Wang, W.Z. Wan, G.M. Tang, Z.W. Qiang, T.D. Li. *J. Coord. Chem.*, **63**, 206 (2010).
- [34] Y.T. Wang, G.M. Tang. *J. Coord. Chem.*, **60**, 2139 (2007).
- [35] N. Kundu, A. Audhya, S.M.T. Abtab, S. Ghosh, E.R.T. Tiekink, M. Chaudhury. *Cryst. Growth Des.*, **10**, 1269 (2010).
- [36] A. Shaukat, H.M. Mirza, A.H. Ansari, M. Yasinzai, S.Z. Zaidi, S. Dilshad, F.L. Ansari. *Med. Chem. Res.*, **22**, 3606 (2012).
- [37] G. Naresh, R. Kant, T. Narender. *J. Org. Chem.*, **79**, 3821 (2014).
- [38] M. Nasr-Esfahani, I. Mohammadpoor-Baltork, A.R. Khosropour, M. Moghadam, V. Mirkhani, S. Tangestaninejad. *J. Mol. Catal. A: Chem.*, **379**, 243 (2013).
- [39] *CrysAlisPro*. Oxford Diffraction, Poland (2009).
- [40] Bruker AXS. *S.AINT Software Reference Manual*. Madison, WI (1998).
- [41] G.M. Sheldrick, *SHELXTL NT Version 5.1. Program for Solution and Refinement of Crystal Structures*, University of Göttingen, Germany (1997).
- [42] G.M. Sheldrick. *Acta Crystallogr., Sect. A: Found. Crystallogr.*, **64**, 112 (2008).
- [43] A.L. Spek. *J. Appl. Cryst.*, **36**, 7 (2003).
- [44] G.R. Desiraju. *Cryst. Growth Des.*, **11**, 896 (2011).
- [45] X.M. Chen, J.W. Cai. *Single-crystal Structural Analysis Principles and Practices*. The Science Press, Beijing (2003).
- [46] D. Sun, L.L. Han, S. Yuan, Y.K. Deng, M.Z. Xu, D.F. Sun. *Cryst. Growth Des.*, **13**, 377 (2013).
- [47] Z. Su, J. Fan, T. Okamura, W.Y. Sun, N. Ueyama. *Cryst. Growth Des.*, **10**, 3515 (2010).
- [48] S.R. Batten. *CrystEngComm*, **18**, 1 (2001).
- [49] S.I. Vasylevs'kyy, G.A. Senchyk, A.B. Lysenko, E.B. Rusanov, A.N. Chernega, J. Jezierska, H. Krautscheid, K.V. Domasevitch, A. Ozarowski. *Inorg. Chem.*, **53**, 3642 (2014).
- [50] R.Q. Zhong, R.Q. Zou, M. Du, T. Yamada, G. Maruta, S. Takeda, J. Li, Q. Xu. *CrystEngComm*, **12**, 677 (2010).
- [51] L.H. Zhao, A.H. Yang, Y.P. Quan, H.L. Gao, J.Z. Cui. *J. Chem. Crystallogr.*, **41**, 1245 (2011).
- [52] Y.L. Wei, J.B. Li, W.C. Song, S.Q. Zang. *Inorg. Chem. Commun.*, **15**, 16 (2012).
- [53] M. Xue, G.S. Zhu, Q.R. Fang, X.D. Guo, S.L. Qiu. *Inorg. Chem. Commun.*, **9**, 603 (2006).
- [54] B. Valeur. *Molecular Fluorescence Principles and Applications*, WILEY-VCH, Weinheim (2002).
- [55] A.C. Tella, S.O. Owolude. *J. Mater. Sci.*, **49**, 5635 (2014).
- [56] J.M. Hao, Y.H. Li, H.H. Li, G.H. Cui. *Transition Met. Chem.*, **39**, 1 (2013).